# Role of multilevel Rydberg interactions in electric-field-tuned Förster resonances

Jorge M. Kondo,[1] Donald Booth,[2] Luís F. Gonçalves,[1] James P. Shaffer,[2] and Luis G. Marcassa[1,*]

[1]*Instituto de Física de São Carlos, Universidade de São Paulo, Caixa Postal 369, 13560-970 São Carlos, São Paulo, Brazil*

[2]*Homer L. Dodge Department of Physics and Astronomy, The University of Oklahoma, 440 West Brooks Street, Norman, Oklahoma 73019, USA*

(Received 23 August 2015; published 8 January 2016)

In this work, we investigate the dc electric-field dependence of two Förster resonant processes in ultracold $^{85}$Rb, $37D_{5/2} + 37D_{5/2} \rightarrow 35L(L = O, Q) + 39P_{3/2}$, as a function of the atomic density. At low densities, the $39P_{3/2}$ yield as a function of electric field exhibits resonances. With increasing density, the linewidths increase until the peaks merge. Even under these extreme conditions, where the Förster resonance processes show little electric-field dependence, the $39P_{3/2}$ population depends quadratically on the total Rydberg atom population, suggesting that a two-body interaction is the dominant process. In order to explain our results, we implement a theoretical model which takes into account the multilevel character of the interactions and Rydberg atom blockade process using only atom pair interactions. The comparison between the experimental data and the model is very good, suggesting that the Förster resonant processes are dominated by two-body interactions up to atomic densities of $3.0 \times 10^{12}$ cm$^{-3}$.

DOI: 10.1103/PhysRevA.93.012703

It is not surprising that a central goal of ultracold Rydberg atom physics has been to investigate many-body physics because important parameters, such as density and interaction strength, can be controlled [1,2]. A significant number of puzzling experimental observations in ultracold Rydberg gases have been explained by invoking many-body effects. Increasing the range of the atom-atom interactions is a natural pathway to study many-body physics. In this context, Förster resonances are the work horses for investigating many-body behavior in ultracold Rydberg gases. Recently, Förster resonances have attracted significant interest in the study of quantum systems driven by classical fluctuations [3], all-optical quantum information processing [4–6], and quantum magnetism [7]. A detailed understanding of Förster resonances in high-density samples is important to these lines of investigation.

Overviews of Förster resonance experiments can be found in several reviews [8–10]. Many works have associated Förster resonance broadening with many-body effects by comparing experimental observation to complex theoretical models. One such many-body model was implemented for the Rb states we study here [11]. More exact theoretical many-body approaches, like quantum Monte Carlo, are difficult to implement in systems of highly excited atoms. A standard approximation involves breaking the multipolar interactions between the atoms into a sum of two-body problems [12–14].

It has been shown that two-body potentials describing interactions between Rydberg atoms are very complex, particularly at short range where many interaction potentials cross. The potentials are sensitive to dc [15] and ac [16] electric fields. Studying a Förster resonance as a function of electric field and atomic density is generally complicated because essential quantities like state to state couplings and Rydberg atom blockade allowed interparticle separations change with applied electric field.

In this paper, we show, based on experiments and calculations of Rydberg atom potentials, that the multilevel character of the Rydberg atom interactions must be considered before concluding that an experimental observation is many body in nature. We define many body here broadly to mean phenomena that involve the interaction of three or more atoms. For a system to exhibit many-body physics, the observables should be attributable to the many-body interactions. A Rydberg atom blockade involves the collective behavior of more than one atom but the atoms do not interact with each other in pure blockade phenomena as the shared excitation prevents further excitation of the atoms within the blockade volume. In this sense, we distinguish purely collective phenomena from many-body interactions although the two are not mutually exclusive.

To demonstrate that the multilevel nature and complexity of Rydberg atom potentials are important for interpreting many-body behavior in ultracold Rydberg gases, we have studied the dc electric-field dependence of two Förster resonance processes for $^{85}$Rb atoms, $37D_{5/2} + 37D_{5/2} \rightarrow 35O(L = 11) + 39P_{3/2}$ and $37D_{5/2} + 37D_{5/2} \rightarrow 35Q(L = 12) + 39P_{3/2}$, as a function of the atomic density. The resonance peaks of the $39P_{3/2}$ state as a function of electric field can be clearly observed at magneto-optical trap (MOT) densities. However, as the density increases, the linewidth of the product yield increases until these peaks merge. Even under these extreme circumstances, where the Förster resonance processes do not show significant variation with electrical field, the $39P_{3/2}$ yield depends quadratically on the total Rydberg state population. As we have shown in our recent work [17], this is strong evidence that a two-body interaction dominates the dynamics. We show that the multistate nature of the Rydberg atom pair interaction potentials [15,18,19] can be used to explain the observed line broadening while maintaining consistency with the quadratic scaling of the product yield with Rydberg state population. The explanation of the line broadening spectra at high densities requires that a Rydberg atom blockade be taken into account [20,21], but does not require the introduction of more than a two-body interaction between a pair of atoms. Such results can

*marcassa@ifsc.usp.br

 

be contrasted with the interpretation proposed in other works appearing in the literature [11,14]. The experimental data and model agree well, suggesting, despite exciting a Förster resonance, that the gas dynamics are dominated by two-body interactions and the complexity of Rydberg interactions can mask the manifestation of many-body interactions.

The experimental setup is described elsewhere [17]. Briefly, a magneto-optical trap is used to load a quasielectrostatic trap (QUEST), producing a nonpolarized atomic sample of $\sim 10^6$ atoms at a peak density of $3.0 \pm 1.0 \times 10^{12}\,\mathrm{cm}^{-3}$ at a temperature of 80 $\mu$K. To probe the Rydberg atom interactions as a function of density, the QUEST is turned off and the sample undergoes free expansion which can vary from 0.1 to 1 ms. The atomic density for different free expansion times was verified by taking absorption images of the expanding atomic cloud. At $t = 0$, the QUEST has a cigar shape with 35-$\mu$m radius and a length of 1450 $\mu$m. The Rydberg excitation occurs after free expansion using two narrow-bandwidth cw laser pulses at $\sim$780 and 480 nm, the duration of which is 700 ns, polarized parallel to the dc electric field. The intensities are $I_{780} = 1.6\,\mathrm{mW\,cm}^{-2}$ and $I_{480} = 80\,\mathrm{W\,cm}^{-2}$, and the respective peak Rabi frequencies are 19 and 29 MHz. To collect the Rydberg atom signal a ramped pulsed electric field is applied 70 ns after the excitation. The electrons are counted on a multichannel plate detector, which gives an average Rydberg atom number of about 15 000. The uncertainty in the dc electric field is estimated to be $\sim 40\,\mathrm{mV\,cm}^{-1}$. The $37D_{5/2}$ and $39P_{3/2}$ populations are observed simultaneously using their arrival time at the detector. We found no evidence of free ions in the experiment. By analyzing the electron signal at early times, we estimate that there are at most four free ions at the highest atomic density.

As in our prior work [17], we use a state-mixing fraction to analyze the population transfer from $37D_{5/2}$ to $39P_{3/2}$, similar to [22]. However, we have defined our state-mixing fraction as twice the $39P_{3/2}$ electron signal divided by the sum of the $37D_{5/2}$ electron signal plus the $39P_{3/2}$ electron signal. The fraction is defined in this way because the $35O$ or $35Q$ electron signal contaminates the $37D_{5/2}$ electron signal in our experiment. The state-mixing fraction calculated in this way can lead to an overestimate of the experimental quantity relative to theory if some of the high $l$ state was not measured in the $37D_{5/2}$ time-of-flight window. In Fig. 1, we show the dc electric-field dependence of the state-mixing fraction as a function of the atomic density. The lowest density measurement was done in a MOT. As the atomic density increases, the linewidth as a function of electric field increases and the peaks, clearly visible at low density, merge. At the highest atomic density, the state-mixing fraction is almost independent of electric field. One might expect to observe many-body effects as this occurs.

A measurement of the atomic density dependence of the $39P_{3/2}$ population will show a power-law dependence higher than 2 if multiparticle interactions are occurring [23]. In the inset of Fig. 1, we show the normalized $39P_{3/2}$ population as a function of normalized total Rydberg atomic population for two different electric fields. One electric field corresponds to off Förster resonance, $1.51\,\mathrm{V\,cm}^{-1}$, and one corresponds to on resonance, $1.61\,\mathrm{V\,cm}^{-1}$. The power-law fit to the total Rydberg atom population, $\rho^{\delta}$, is clearly second order as

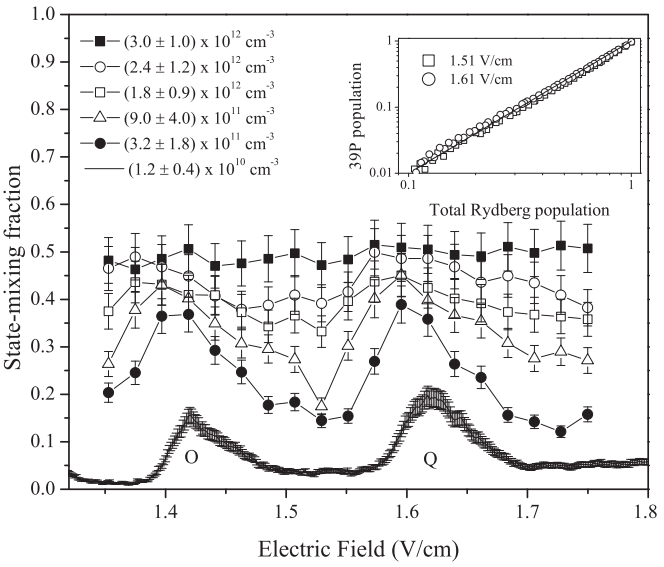


FIG. 1. State-mixing fraction as a function of dc electric field as a function of the atomic density. The resonances involving $L = O, Q$ are labeled. In the inset, we show the normalized $39P_{3/2}$ population as a function of the normalized total Rydberg atomic population for two different electric fields, off resonance at $1.51\,\mathrm{V\,cm}^{-1}$ and on resonance at $1.61\,\mathrm{V\,cm}^{-1}$.

$\delta = 2.0 \pm 0.1$. It is clear from this straightforward data and analysis that the observed Förster resonance process is the result of a two-body effect.

To explain the population transfer to $39P_{3/2}$, we calculated Rydberg atom interaction potential curves for $37D_{5/2} + 37D_{5/2}$ at fields around $1.65\,\mathrm{V\,cm}^{-1}$ and performed an analysis on these potential curves to determine the expected line shapes and product yields at various ground-state atomic densities. At a field of $1.65\,\mathrm{V\,cm}^{-1}$ ($1.45\,\mathrm{V\,cm}^{-1}$), the asymptote corresponding to $39P_{3/2} + 35Q$ ($39P_{3/2} + 35O$) is degenerate with the $37D_{5/2} + 37D_{5/2}$ asymptote, enabling strong interactions which can result in population transfer. There is a small discrepancy between the experimental peak ($\sim 1.61\,\mathrm{V\,cm}^{-1}$) and the theoretical one ($\sim 1.65\,\mathrm{V\,cm}^{-1}$). The offset may be due to the small background electric field and/or a small offset resulting from the quantum defects used to calculate the energy levels. The interaction potential calculation for this system must include all $L$ states up to $L = (n - 1)$ [15]. For the $37D_{5/2} + 37D_{5/2}$ system we calculated potentials and eigenvectors at fields varying from 1.35 to $1.65\,\mathrm{V\,cm}^{-1}$ in intervals of $0.025\,\mathrm{V\,cm}^{-1}$. At each of these fields we used the potentials and eigenvectors to calculate a line shape for the $37D_{5/2}$ and $39P_{3/2}$ signals.

In prior work [17], we have demonstrated that a saturation behavior, which has been previously attributed to many-body effects [22], is actually a manifestation of the blockade effect due to two interacting atoms in a high-density sample. We have verified that the $37D_{5/2}$ population saturates as the atomic density increases, consistent with the existence of a Rydberg atom blockade process. From this measurement, we are able to measure a Rydberg atom blockade radius of 5.3 $\mu$m.

We calculate an absorption coefficient taking into account the saturation effects caused by the Rydberg atom blockade to calculate the line shape for the $37D_{5/2} + 37D_{5/2}$ signal and

the $39P_{3/2}$ product yield. We use an absorption coefficient based on those found in [24,25] as the starting point for the calculation:

$$\alpha(E) = \frac{\rho e^2 \pi}{4c\epsilon_0 m_e} \sum_{a=1}^{3} \frac{\sigma/2\pi}{\sigma^2 + \left(E_{dd_a} - E\right)^2} \tag{1}$$

$$\int_0^\infty \sum_i^{\text{all states}} P_{\text{pair}}(R) p_i(R) R^2 dR. \tag{2}$$

$p_i(R)$ is the excitation probability into the $37D_{5/2} + 37D_{5/2}$ asymptotes $E_{dd_a}$, including each projection on the internuclear axis. For the $39P_{3/2}$ yield, the excitation probability contains an additional term indicating the overlap between $37D_{5/2} + 37D_{5/2}$ and $35O + 39P_{3/2}$ and $35Q + 39P_{3/2}$, $p_i(R) = p_P(R)p_D(R)$. $e$ is the charge of the electron, $\rho$ is the trap density, and $m_e$ is the mass of the electron. Since there is an applied electric field, the $m_J$ sublevels of $37D_{5/2} + 37D_{5/2}$ split, so it is important to account for each asymptote, $a$. $E$ is the energy of the photon. $\sigma$ is the spectral linewidth including the laser linewidth and the linewidth of $5P_{3/2}$. $P_{\text{pair}}$ is the pair-state correlation function [18]. At the laser intensities and densities used in the experiment, saturation must be considered. The spectral line shape with saturation is [26]

$$\alpha_{\text{sat}}(E) = \frac{\alpha(E)}{1 + S_E}, \tag{3}$$

where

$$S_E = \eta(\rho) \frac{B_{12}\rho_s(E)}{\Gamma} L\left(E_{dd_a} - E\right). \tag{4}$$

$B_{12}$ is the Einstein coefficient of induced absorption, $\rho_s(E)$ is the spectral energy density of the excitation light, $\Gamma$ is the mean relaxation rate, $\eta(\rho)$ is the hard sphere model parameter [27], and

$$L(E_{dd_a} - E) = \alpha(E) \frac{4c\epsilon_0 m_e}{\rho e^2 \pi} \tag{5}$$

is the line-shape function. The density-dependent hard-sphere model treats the system as spheres around the Rydberg atoms in which further excitation is forbidden. The hard-sphere model accounts for the saturation of the line shape due to the Rydberg atom blockade. The region of electric fields between the crossings of $37D_{5/2} + 37D_{5/2}$ and $35O + 39P_{3/2}$ and $37D_{5/2} + 37D_{5/2}$ and $35Q + 39P_{3/2}$ was modeled and compared to experimental data.

The first test of the model is a comparison of the predicted frequency dependent excitation and product yield line shapes obtained experimentally in a complementary experiment. The $37D_{5/2}$ and $39P_{5/2}$ populations were measured as a function of the Rydberg excitation laser frequency on the Förster resonance at 1.61 V cm$^{-1}$ (Fig. 2). The trap density is $3 \times 10^{12}$ cm$^{-3}$. The agreement between theory and experiment is very good. We point out that (i) the model is able to reproduce the $39P_{3/2}/37D_{5/2}$ population ratio with no free parameter; (ii) the small disagreement on the red side of the excitation line shape can be explained by the fact that the light polarization is not pure; and (iii) if the Rydberg atom blockade effect is neglected, the $37D_{5/2}$ state population almost doubles around

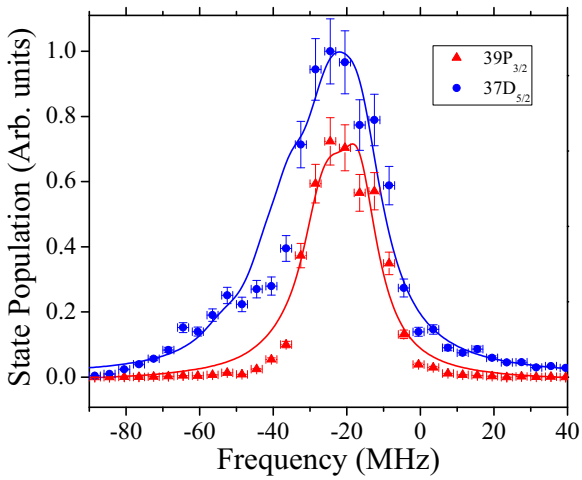


FIG. 2. $37D_{5/2}$ and $39P_{3/2}$ state normalized populations as a function of the Rydberg excitation laser frequency on the Förster resonance at 1.61 V cm$^{-1}$. The $37D_{5/2}$ state population shows saturation behavior, which is due to the Rydberg atom blockade. The points are the experimental data and the line is the theoretical model. The density for this measurement is $3 \times 10^{12}$ cm$^{-3}$. The signals are normalized to the peak $37D_{5/2}$ signal. No other free parameters are used to generate the theoretical graphs. The frequency zero is set at the $37D_{5/2}$ atomic resonance at zero electric field.

the resonance, showing that there is a strong saturation effect. The line shape depends on the $m_J$ of the asymptotic pair and thus the polarization of the excitation light. The structure observed in the line shape is largely due to the splitting of the asymptotic pair states correlating to different $m_J$. We modeled the absorption line shapes with the polarization to which the lasers were set. Polarization impurity can be introduced at the trap because of birefringence in the vacuum chamber windows and other optics. Rather than fitting the line shape to a variable degree of ellipticity, we leave this effect as a systematic error to present the analysis without the elipticity as a free parameter.

In a second test, we reproduced the dc electric-field dependence of the Förster resonance processes as a function of the atomic density. Figure 3 shows the experimental and calculated state-mixing fraction as a function of electric field with a constant excitation laser detuning of 0 MHz from $37D_{5/2} + 37D_{5/2}$ at zero electric field at densities of $1.2 \times 10^{10}$, $3.2 \times 10^{11}$, $9.0 \times 10^{11}$, $1.8 \times 10^{12}$, $2.4 \times 10^{12}$, and $3 \times 10^{12}$ cm$^{-3}$. As the density increases, the lines broaden and the state-mixing fraction saturates to $\sim$0.4 . At low density, the linewidth is due to a convolution of the (i) laser and state linewidths and (ii) multilevel nature of the potentials and the pair distribution function. The model predicts the linewidth for $1.2 \times 10^{10}$ cm$^{-3}$ primarily taking into account two-body interactions. At high atomic density, the sample is blockaded. Outside the blockade radius the pair distribution function is basically constant and $p_i(R)$ has weak radial and electric-field dependence.

The interpretation of these results is fairly straightforward. The system is dominated by pair interactions when the density is low enough so that interacting atoms are only excited in the asymptotic region where the interactions are weak. A third atom is, on average, so far away from an interacting pair of atoms that there is no significant three-body or higher inter-

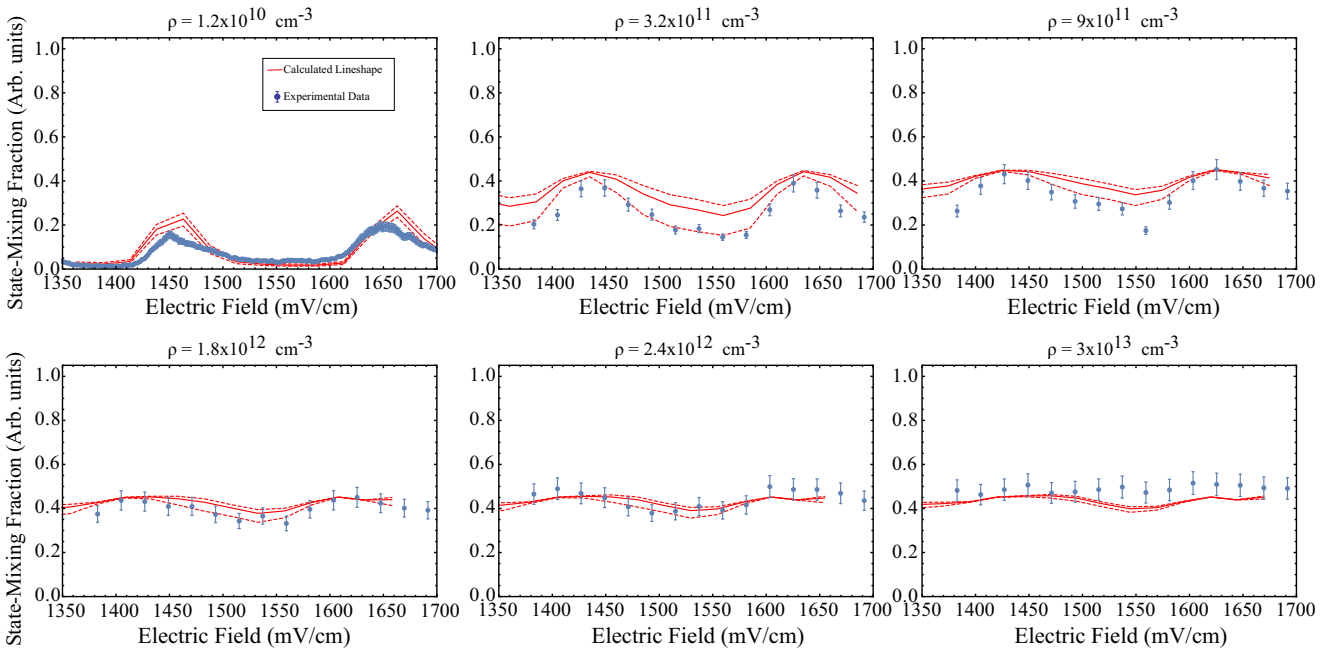


FIG. 3. Experimental and calculated state-mixing fraction as a function of electric field, with an excitation laser detuning of 0 MHz from the $37D_{5/2}$ resonance at densities ranging from $1.2 \times 10^{10}$ to $3 \times 10^{12}$ cm$^{-3}$. Two resonances appear in the density range shown; as the density is increased these resonances merge. The dashed lines represent the lower and upper boundary of the atomic density uncertainty.

action. As the density increases, the Rydberg atom blockade prevents excitations from getting close enough to each other to begin to have significant three-body or higher interactions. The multilevel nature of the Rydberg atom interaction potentials is more important than higher-order interactions for explaining the line shapes. The multilevel interaction potentials calculated in the electric field also tend to be weaker than what one would anticipate when these effects are not considered, at least around the $37D_{5/2} + 37D_{5/2}$ asymptote. Using idealized interaction potentials overestimates the strength of the interactions. Note that relatively weak excitation laser fields were used for our experiments. The multilevel effects explained here can also become relevant in strong laser fields [16].

In conclusion, we have studied the Förster resonance processes $37D_{5/2} + 37D_{5/2} \rightarrow 35O + 39P_{3/2}$ and $37D_{5/2} + 37D_{5/2} \rightarrow 35Q + 39P_{3/2}$. We provided evidence that the broadening is not a many-body or even few-body effect. To explain our results, we implemented a model based on the multilevel character of two-body interactions and a Rydberg atom blockade. The model fits the experimental results well, supporting the explanation that the Förster resonance process, at least in this case, is dominated by a two-body interaction. The complexity of Rydberg interactions can mask the manifestation of many-body behavior. Many-body or multiparticle effects should be proved through straightforward density scalings [23] or other clear signatures such as nonlinear response.

This work is supported by Grants No. 2012/19342-6 and No. 2013/02816-8, São Paulo Research Foundation (FAPESP), AFOSR (Grant No. FA9550-12-1-0434), NSF (Grant No. PHY-1205392), and INCT-IQ and CNPq.

[1] W. R. Anderson, J. R. Veale, and T. F. Gallagher, Phys. Rev. Lett. **80**, 249 (1998).
[2] I. Mourachko, D. Comparat, F. de Tomasi, A. Fioretti, P. Nosbaum, V. M. Akulin, and P. Pillet, Phys. Rev. Lett. **80**, 253 (1998).
[3] M. Sarovar and M. D. Grace, Phys. Rev. Lett. **109**, 130401 (2012).
[4] D. Paredes-Barato and C. S. Adams, Phys. Rev. Lett. **112**, 040501 (2014).
[5] D. Tiarks, S. Baur, K. Schneider, S. Dürr, and G. Rempe, Phys. Rev. Lett. **113**, 053602 (2014).
[6] D. Barredo, H. Labuhn, S. Ravets, T. Lahaye, A. Browaeys, and C. S. Adams, Phys. Rev. Lett. **114**, 113002 (2015).
[7] R. M. W. van Bijnen and T. Pohl, Phys. Rev. Lett. **114**, 243002 (2015).
[8] D. Comparat and P. Pillet, J. Opt. Soc. Am. B **27**, A208 (2010).
[9] T. F. Gallagher and P. Pillet, in *Advances in Atomic, Molecular and Optical Physics*, Advances In Atomic, Molecular, and Optical Physics Vol. 56, edited by E. Arimondo, P. R. Berman, and C. C. Lin (Academic, New York, 2008), p. 161.
[10] L. G. Marcassa and J. P. Shaffer, in *Advances in Atomic, Molecular and Optical Physics*, Advances In Atomic, Molecular, and Optical Physics Vol. 63, edited by E. Arimondo, P. R. Berman, and C. C. Lin (Academic, New York, 2014), p. 47.
[11] E. Altiere, D. P. Fahey, M. W. Noel, R. J. Smith, and T. J. Carroll, Phys. Rev. A **84**, 053431 (2011).

[12] J. V. Hernandez and F. Robicheaux, J. Phys. B **39**, 4883 (2006).
[13] B. Sun and F. Robicheaux, Phys. Rev. A **78**, 040701 (2008).
[14] T. J. Carroll, S. Sunder, and M. W. Noel, Phys. Rev. A **73**, 032725 (2006).
[15] A. Schwettmann, J. Crawford, K. R. Overstreet, and J. P. Shaffer, Phys. Rev. A **74**, 020701 (2006).
[16] V. A. Nascimento, L. L. Caliri, A. Schwettmann, J. P. Shaffer, and L. G. Marcassa, Phys. Rev. Lett. **102**, 213201 (2009).
[17] J. M. Kondo, L. F. Gonçalves, J. S. Cabral, J. Tallant, and L. G. Marcassa, Phys. Rev. A **90**, 023413 (2014).
[18] J. S. Cabral, J. M. Kondo, L. F. Gonçalves, L. G. Marcassa, D. Booth, J. Tallant, and J. P. Shaffer, New J. Phys. **12**, 093023 (2010).
[19] J. S. Cabral, J. M. Kondo, L. F. Gonçalves, V. A. Nascimento, L. G. Marcassa, D. Booth, J. Tallant, A. Schwettmann, K. R. Overstreet, J. Sedlacek, and J. P. Shaffer, J. Phys. B **44**, 184007 (2011).
[20] M. Robert-de-Saint-Vincent, C. S. Hofmann, H. Schempp, G. Günter, S. Whitlock, and M. Weidemüller, Phys. Rev. Lett. **110**, 045004 (2013).
[21] C. Ates, S. Sevinçli, and T. Pohl, Phys. Rev. A **83**, 041802 (2011).
[22] K. C. Younge, A. Reinhard, T. Pohl, P. R. Berman, and G. Raithel, Phys. Rev. A **79**, 043420 (2009).
[23] J. H. Gurian, P. Cheinet, P. Huillery, A. Fioretti, J. Zhao, P. L. Gould, D. Comparat, and P. Pillet, Phys. Rev. Lett. **108**, 023005 (2012).
[24] J. Stanojevic, R. Côté, D. Tong, E. E. Eyler, and P. L. Gould, Phys. Rev. A **78**, 052709 (2008).
[25] J. Deiglmayr, H. Saßmannshausen, P. Pillet, and F. Merkt, Phys. Rev. Lett. **113**, 193001 (2014).
[26] W. Demtröder, *Laser Spectroscopy: Basic Concepts and Instrumentation*, 3rd ed. (Springer-Verlag, New York, 2003).
[27] C. S. Hofmann, Ph.D. thesis, University of Heidelberg, 2013.